Transition Energy Crossing in NICA Collider of Polarized Proton Beam in Harmonic and Barrier RF

S. D. Kolokolchikov[a,b,*], **A. E. Aksentev**[a,b,c], **A. A. Mel'nikov**[a,b,d], **and Yu. V. Senichev**[a,b]

[a] *Institute of Nuclear Research, Russian Academy of Sciences, Moscow, 117312 Russia*
[b] *Moscow Institute of Physics and Technology (National Research University), Dolgoprudny, Moscow oblast, 141701 Russia*
[c] *National Research Nuclear University MEPhI (Moscow Engineering Physics Institute), Moscow, 115409 Russia*
[d] *Landau Institute of Theoretical Physics, Russian Academy of Sciences, Chernogolovka, Moscow oblast, 142432 Russia*
*e-mail: sergey.bell13@gmail.com

Abstract—The present study explores the application transition energy jump procedure in order to maintain the stability of the beam in the NICA collider. The features of the barrier and harmonic accelerating RF stations and their influence on the dynamics of longitudinal particle motion are described. Study of these features is intended to expand the understanding of the process of transition energy crossing.

INTRODUCTION

The problem of transition energy crossing in the NICA synchrotron at the Joint Institute of Nuclear Energy in Dubna, Moscow oblast, is relevant for experiments with protons at a beam energy of 13 GeV, since it can increase emittance and ultimately imposes restrictions on the resulting luminosity. Such problems do not arise for experiments with heavy ions at an energy of 4.5 GeV because the transition energy is 5.7 GeV.

Using the transition energy jump procedure in the NICA with a betatron tune shift limits the magnitude of the jump. The limited rate of quadrupole gradients change results in a limited rate of change in the transition energy. A similar jump scheme has been considered for accelerating RF stations (barrier and harmonic) that differ by their operating principle. The scheme has also been compared to the transition energy jump procedure on the U-70 accelerator at IHEP in Protvino, Moscow oblast.

LUMINOSITY

Luminosity is a key value in a collider experiment. In the simplest case (the colliding of symmetric bunches), luminosity is given by the formula [1]

$$L = \frac{n_{\text{bunch}} N_1 N_2 f_0}{4\pi\sqrt{\varepsilon_x \varepsilon_y} B^*} \Phi_{\text{HG}},$$

$$\Phi_{\text{HG}}(\alpha) = \frac{2}{\sqrt{\pi}} \int_0^\infty \sigma_s \frac{e^{-u^2} du}{1 + (\alpha u)}, \quad \alpha = \frac{\sigma_s}{B^*}, \tag{1}$$

where n_{bunch} is the number of bunches, N_1, N_2 is the number of particles in colliding bunches, $\varepsilon_x, \varepsilon_y$ are the transverse emittances, f_0 is the revolution frequency, Φ_{HG} is the hourglass parameter, σ_s is the Gaussian parameter of the longitudinal size, and B^* is the beta function at the point of collision. We can see this formula represents the fundamental dependence on many parameters of both the beam and magneto-optics.

Transition energy crossing strongly affects the longitudinal dynamics. The luminosity depends explicitly on the longitudinal length of the beam only through the hourglass parameter $\Phi_{\text{HG}}(1) \cong 0.76$, $\Phi_{\text{HG}}(2) \cong 0.55$, and $\Phi_{\text{HG}}(5) \cong 0.29$, i.e., with constant parameters and only a doubling of bunch length, the influence of the hourglass effect reduces the initial luminosity by 30%. For the NICA, it is expected to reach $\alpha = 1$, $\sigma_s = 0.6$ m. The beta function at the point of collision is $B^* = 0.6$ m, so only the explicit dependence on the longitudinal length is considered. The luminosity depends implicitly on the longitudinal emittance of the bunch, since it sets a limit on the number of particles.

ACCELERATION

Let us now consider the evolution of longitudinal emittance during acceleration in a barrier RF. To achieve luminosity on the order of 2×10^{32} cm^{-2} s^{-1},
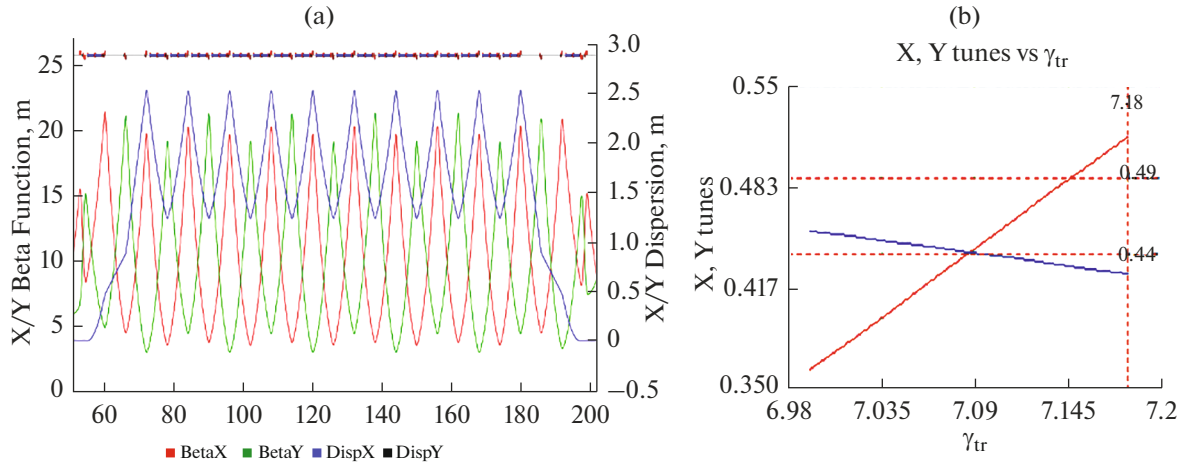
Fig. 1. (a) Twiss parameters β_x, β_y, D_x of the NICA bending arc; (b) dependence of the betatron frequency in plane x, y on γ_{tr} when the dispersion function is modulated by changing the gradient in the focusing lenses.

the final rms normalized longitudinal emittance of the bunch is $\varepsilon_{sin}^{exp} = n_{bunch}\gamma_{exp}\beta_{exp}\pi\sigma_s\sigma_p = 0.9$ m ($\gamma_{exp} = 14.3$, $n_{bunch} = 22$, $\sigma_s = 0.6$ m, $\sigma_p = 1.5\times10^{-3}$) at an energy on the order of 13 GeV.

It is formed from the emittance of a uniform bunch in a barrier RF, divided into 22 bunches using RF gymnastics. The emittance of a barrier RF is affected by the influence of the transition energy on the emittance of the cooled beam after injection, $\varepsilon_{bb}^{cool} \cdot \varepsilon_{bb}^{fin} = D_{tr}\varepsilon_{bb}^{cool}$. The cooled beam is formed after injection, accumulation, and electron cooling by 2–3 GeV $\varepsilon_{bb}^{cool} = D_{cool}\varepsilon_{bb}^{in\,j}$. Cooling alone reduces emittance $D_{cool} < 1$; the other effects only inflate emittance $D_{gym} > 1$, $D_{tr} > 1$. For gymnastics, $D_{gym} = 1.3$. The influence of D_{tr} is discussed below.

TRANSITION ENERGY JUMP

The transition energy jump procedure is used to preserve the phase volume. A jump in transition energy caused by shifting the betatron tunes is being considered for the NICA. The parameters of the jump can be determined by studying its magneto-optical structure and the possibility of changing the current in the quadrupole lenses in the bending arcs.

The change in transition energy is achieved by changing the mometum compaction factor:

$$\alpha = \frac{1}{C}\int_0^C \frac{D(s)}{\rho(s)}ds, \qquad (2)$$

where $D(s)$ is the dispersion function and $\rho(s)$ is the curvature of the orbit. Modulation of the dispersion function is required. The magneto-optical structure of the NICA's bending arcs consists of 12 FODO cells

with dispersion suppressed at their edges (Fig. 1a). The MADX [2] and OptiM [3] programs for numerically modeling the motion of the beam in the magnetic systems of accelerators were used to study the dependence of the change in the transition energy on the tune of betatron oscillations. The gradient in the focusing quadrupole lenses also changed. It is in these elements that the maxima of β_x and D_x are located. In the existing structure, $\Delta\gamma_{tr} = 1.1\Delta q$ (Fig. 1b). To ensure a jump on the order of $\Delta\gamma_{tr} = 0.09$, we must change the frequency within the range of $\Delta\gamma_{tr} = 1.1\Delta q$. The corresponding total change in the gradient is $\Delta Kl = 4\pi\Delta q/\beta_a = 0.055$ m^{-1}, where $\beta_a = 11.5$ m is the average beta function.

The maximum change in the gradient in one quadrupole is then $\Delta G = \Delta Kl(BR/N_F l) = 0.5$ T/m, where $N_F = 24$ is the number of focusing lenses, $BR = 22$ T m is the magnetic rigidity at a proton kinetic energy of 5.7 GeV (the transition energy), and $l = 0.47$ m is the length of the quadrupole. Limiting the rate of current increase limits the change in the gradient of the quadrupole lenses. The rate of change in the transition energy is $d\gamma_{tr}/dt = 8.5$ s^{-1} [4].

The transition energy jump procedure is also used in the U-70, the proton synchrotron operated by the Kurchatov Institute (IHEP) [5]. The magneto-optical structure of the U-70 is FODO-periodic and consists of 12 superperiods containing 10 magnetic blocks with a combined function [6]. Acceleration is done using harmonic RF with a rate of $(d\gamma/dt)_{U-70} = 40$ s^{-1}. The jump is also achieved by distorting the dispersion function without shifting the operating point. Additional quadrupoles placed every half period $\Delta\nu_{x,y} = 0.5\times 0.5$ and having opposite polarities mod-
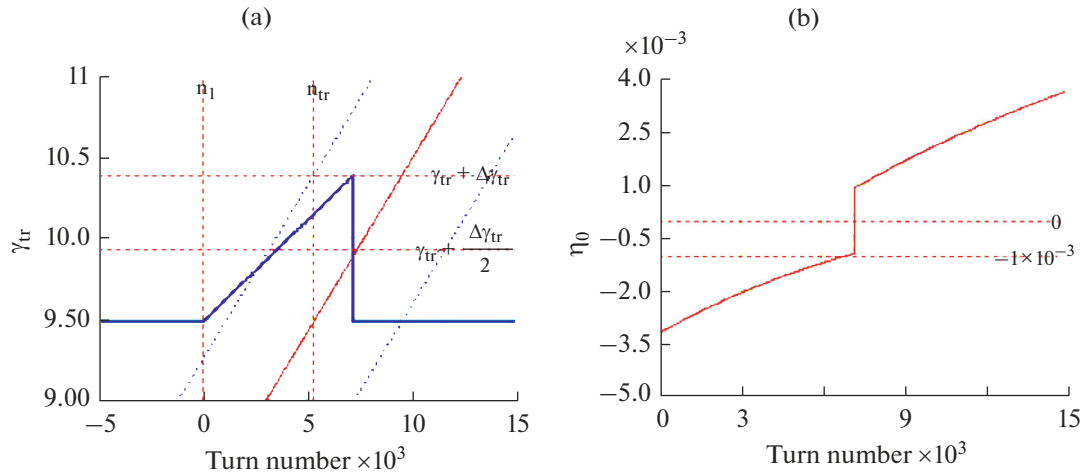
Fig. 2. (a) Schematic diagram of the rise in transition energy on U-70 during the jump procedure at $\Delta\gamma_{tr}^{U-70} = 0.9$ with rate $(d\gamma_{tr}/dt)_{U-70} = 900 \text{ s}^{-1}$; (b) the corresponding first-order change in slip-factor η_0.

ulate the dispersion function. The transition energy changes at $\Delta\gamma_{tr}^{U-70} = 0.9$ (Fig. 2a) in 1 ms; i.e., 10 times more and 100 times faster than the above jump for the NICA: $(d\gamma_{tr}/dt)_{U-70} = 900 \text{ s}^{-1}$. Corresponding change $\eta_0 = \alpha_0 - \dfrac{1}{\gamma^2}$, where γ is the Lorentz factor of the beam [7], is also shown (Fig. 2b).

The rate of acceleration directly affects the dynamics of longitudinal motion. Three different types of RF stations are installed in the NICA: RF-1, the barrier station, and four RF-2 and eight RF-3 stations that have harmonics with numbers of 22 and 66, respectively. The maximum total voltage is on the order of $(d\gamma/dt)_{RF2} = 30 \text{ s}^{-1}$, $(d\gamma/dt)_{RF3} = 300 \text{ s}^{-1}$ and is much higher than the one used for inductive acceleration in the barrier: $(d\gamma/dt)_{RF1} = 0.2 \text{ s}^{-1}$ [8].

HARMONIC RF

Acceleration in the harmonic RF cavity is achieved by shifting the phase of the beam relative to that of the RF. The rate of acceleration in the harmonic RF-2, $(d\gamma/dt)_{RF2} = 30 \text{ s}^{-1}$, is greater than the maximum rate of change in the transition energy, $d\gamma_{tr}/dt = 8.5 \text{ s}^{-1}$.

Figure 3a shows the scheme of a symmetrical jump from $\gamma_{tr} + \Delta\gamma_{tr}/2$ to $\gamma_{tr} - \Delta\gamma_{tr}/2$. A preliminary increase in the transition energy and the corresponding restoration to the stationary value can in this case occur not with the maximum rate of change in the transition energy, but more slowly. The time spent near the zero value of η is therefore reduced. The slip-factor changes slowly during a jump, compared to one in the U-70 (Fig. 3b). A long stay near the zero value is hazardous for the longitudinal dynamics of the

beam, which is why a jump in (a fast crossing of) the transition energy is applied. Due to the limited magnitude of the jump itself, $\Delta\gamma_{tr} = 0.09$, and the limited rate of change in the transition energy, $d\gamma_{tr}/dt = 8.5 \text{ s}^{-1}$, the jump itself is negligible.

BARRIER RF

Barrier RF-1 generates 5 kV barrier pulses to hold the beam; acceleration is achieved inductively, using a meander with a voltage of 300 V [8]. Rate of acceleration $(d\gamma/dt)_{RF1} = 0.2 \text{ s}^{-1}$ is much slower than the harmonic rate (Fig. 4a). The jump occurs at the same time (10 ms) as with a harmonic RF. The longitudinal dynamics in such RFs differs from those of a harmonic, where $\eta_0 = -2.5 \times 10^{-4}$ reaches a low value and is kept there; nonlinearity $\eta = \eta_0 + \eta_1\delta$ than affects particles with a large δ. However, this is not hazardous for a barrier RF, since there is no additional excitation that can push particles outside the separatrix and distort the distribution between the barriers. The beam profile has a nonzero gradient only at the edges, where particles are reflected from the barrier. Once the transition energy is raised, a jump occurs in 10 ms when there are no barriers. The phase portrait changes negligibly during this time, and we observe capture by barriers with reverse polarity.

It is of greatest importance that the possible value of a jump ($\Delta\gamma_{tr} = 0.09$) and the rate of change in the transition energy ($d\gamma_{tr}/dt = 8.5 \text{ s}^{-1}$) are limited. The limit on the jump also restricts that of the slip-factor ($\eta_0 = \pm 2.5 \times 10^{-4}$). The barrier RF ensures relatively long retention of the beam in the vicinity of the zero value of η_0 (Fig. 4b).
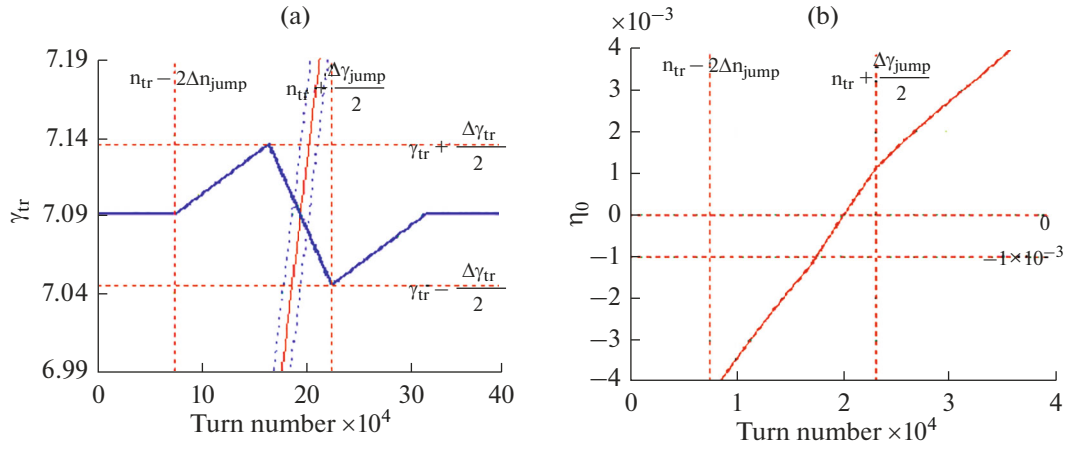
Fig. 3. (a) Schematic diagram of the increase in transition energy at the NICA in the harmonic RF with a rate of $(d\gamma/dt)_{RF2} = 30$ s^{-1} during the jump procedure: $\Delta\gamma_{tr} = 0.09$ with rate $d\gamma_{tr}/dt = 8.5$ s^{-1}; (b) the corresponding first-order change in slip-factor $\eta_0 = \pm 1 \times 10^{-3}$.

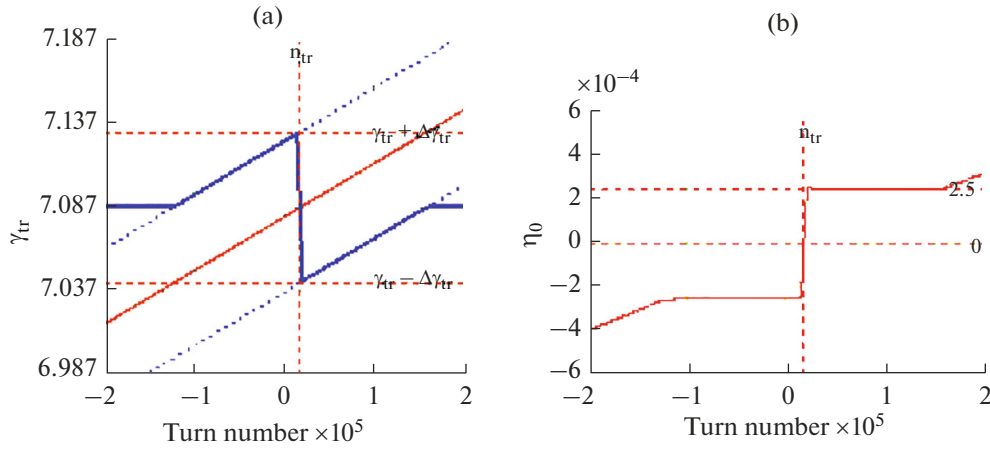**Fig. 4.** (a) Schematic diagram of the increase in transition energy at the NICA in a barrier RF with rate $(d\gamma/dt)_{RF1} = 0.2$ s^{-1} during the jump procedure: $\Delta\gamma_{tr} = 0.09$ with rate $d\gamma_{tr}/dt = 8.5$ s^{-1}; (b) the corresponding first-order change in slip-factor $\eta_0 = \pm 2.5 \times 10^{-4}$.

LONGITUDINAL MICROWAVE INSTABILITY

The limit on the threshold of microwave instability depends on many parameters. For the uniform distribution typical of barrier RFs, it is determined by the Keil−Schnell criterion. The criterion was presented in a modified form in [9]:

$$K_1 K_2 \frac{E_0}{(|Z_\parallel|/n)\, I} \frac{A_i}{Z_i} \gamma\beta^2 |\eta| \sigma_p^2 \geq 1. \qquad (3)$$

Current $I = \dfrac{e\beta c N_p Z_i}{L_B}$, where L_B is the beam length for a barrier RF. This is approximately the distance between the barriers if we ignore edge effects. The for-

mula clearly shows there is a limit on the number of particles (for protons):

$$N_p \leq K_1 K_2 \frac{E_0}{(Z_\parallel/n)ec} |\eta|\, \gamma\beta\sigma_p^2 L_B. \qquad (4)$$

Since the normalized emittance for a barrier RF is $\varepsilon_{tr} = \gamma_{tr}\beta_{tr}\sqrt{\pi}\sigma_p L_B$ (with factor $\sqrt{\pi}$, since the pulse distribution has a Gaussian form and the longitudinal size is uniform), for a barrier RF we have

$$N_p \leq K_1 K_2 \frac{E_0}{(Z_\parallel/n)ec} |\eta| \frac{\varepsilon_{tr}^2}{\pi\gamma\beta L_B}. \qquad (5)$$
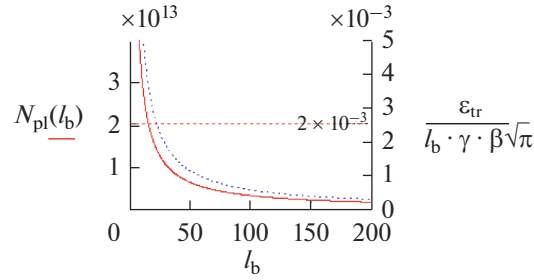
Fig. 5. Dependence of the number of particles in a barrier RF and the momentum spread on the length between the barriers from the viewpoint of longitudinal microwave instability.

The number of particles is thus limited by the length of the bunch in a barrier RF near a low value of $|\eta|$. The normalized emittance is determined by the requirement to have sufficient luminosity $\varepsilon_{tr} = \varepsilon_{bb}^{fin} = \dfrac{\varepsilon_{sin}^{exp}}{D_{gym}} = 0.7$ m, while the length of the bunch can be varied by moving the barriers.

The number of particles required to achieve luminosity on the order of 2×10^{32} cm^{-2} s^{-1} is $N_{exp} = 1 \times 10^{12}$ for the final bunch, so the required number of particles in a barrier RF must be no less than 2.2×10^{13}. For the above jump, energy $E_0 = E_{tr} = 5.7$ GeV, $\gamma_{tr} = 7.08$, $\beta = 0.99$ near $|\eta_0| = 2.5 \times 10^{-4}$. For calculations, we use $Z_\parallel/n = 20\ \Omega$, $K_1 = 1$, and $K_2 = 5.4$

$$N_p \le 1 \times 5.4 \frac{5.7 \times 10^9 \text{ eV}}{20\ \Omega\ 1.6 \times 10^{-19} \text{ C } 3 \times 10^8 \text{ m/s}}$$

$$\times \left|2.5 \times 10^{-4}\right| \frac{(0.7 \text{ m})^2}{7.08 \pi L_B}.$$

This dependence is plotted in Fig. 5. The limit on beam length $L_B = C_{ring}/2$ is thus the limit on the number of particles $N_p \le 1.2 \times 10^{12}$. For $L_B = C_{ring}/10$, $N_p \le 6 \times 10^{12}$.

Based on these estimates, obtaining finite number of particles $N_{exp} = 1 \times 10^{12}$ for each of the 22 bunches seems to be a challenging task, due to longitudinal microwave instability near the transition energy for an intense uniform bunch in a barrier RF.

CONCLUSIONS

Collider experiments mainly impose requirements for their luminosity that restrict, among other things, the longitudinal phase volume of the final bunch. During acceleration, we must overcome the transition energy and divide the beam into 22 bunches using RF gymnastics, without inflating the phase volume.

A possible scheme for the jump in transition energy was considered for the NICA. The characteristic quantities are jump value $\Delta\gamma_{tr} = 0.09$ and the rate of change in transition energy $d\gamma_{tr}/dt = 8.5$ s^{-1}. The proposed jump has little effect on the longitudinal dynamics for harmonic RF, due to the smallness of the jump and its low rate, compared to that of acceleration. For a barrier RF, the limit on the jump size yields a threshold value for the number of particles in a uniform bunch. This is due to microwave instability and prevents us from reaching 1×10^{12}, the number of particles in the final bunch needed to achieve maximum luminosity.

CONFLICT OF INTEREST

The authors of this work declare that they have no conflicts of interest.

REFERENCES

1. I. N. Meshkov, Phys. Part. Nucl. **50**, 663 (2019).
   https://doi.org/10.1134/S1063779619060042

2. MADX. https://mad.web.cern.ch/mad/.

3. V. Lebedev, OptiM code. Private communication.
   www-bdnew.fnal.gov/pbar/organizationalchart/lebedev/OptiM/optim.htm.

4. E. M. Syresin, A. V. Butenko, P. R. Zenkevich, O. S. Kozlov, S. D. Kolokolchikov, S. A. Kostromin, I. N. Meshkov, N. V. Mityanina, Yu. V. Senichev, A. O. Sidorin, and G. V. Trubnikov, Phys. Part. Nucl. **52**, 997 (2021).
   https://doi.org/10.1134/S1063779621050051

5. P. T. Pashkov, *Fundamentals of Proton Synchrotron Theory: A Textbook for Students of the Lomonosov Moscow*

State University (Institut Fiziki Vysokikh Energii, Protvino, Moscow oblast, 1999).

6. S. A. Chernyi, Fiz. Elem. Chastits At. Yadra **22**, 1067 (1991).

7. S. D. Kolokolchikov, Yu. V. Senichev, and V. A. Kalinin, Phys. At. Nucl. **87** (10), 1355 (2024).

8. A. G. Tribendis, Y. A. Biryuchevsky, O. I. Brovko, K. N. Chernov, A. N. Dranitchnikov, E. Kenzhebulatov, A. A. Kondakov, A. A. Krasnov, Ya. G. Kruchkov, S. A. Krutikhin, G. Y. Kurkin, A. M. Malyshev, A. Yu. Martynovsky, I. N. Meshkov, N. V. Mityanina, S. V. Motygin, A. A. Murasev, V. N. Osipov, V. M. Petrov, E. Pyata, E. Rotov, E. Syresin, V. V. Tarnetsky, I. A. Zapryagaev, A. A. Zhukov, and A. V. Zinkevich, in *Proceedings of the IPAC'21, Campinas, Brazil, 2021*, International Particle Accelerator Conference, Vol. 12 (JACoW Publishing, Geneva, 2021), p. 1136.

https://doi.org/10.18429/JACoW-IPAC2021-MOP-AB365

9. S. Kolokolchikov, Yu. Senichev, A. Aksentev, A. Melnikov, V. Ladygin, and E. Syresin, Phys. Part. Nucl. Lett. **21**, 419 (2024).
https://doi.org/10.1134/S1547477124700389

10. P. R. Zenkevich, Investigation of the Stability of Intense Proton Beams in the NICA Collider. Report (2019).

Translated by M. Shmatikov